β-delayed γ decay of ^{26}P: Possible evidence of a proton halo

D. Pérez-Loureiro *et al.*

Phys. Rev. C **93**, 064320 — Published 20 June 2016

DOI: 10.1103/PhysRevC.93.064320

β–delayed γ–decay of ^{26}P: Hint of a proton halo

D. Pérez-Loureiro,[1,*] C. Wrede,[1,2,†] M. B. Bennett,[1,2] S. N. Liddick,[1,3] A. Bowe,[1,2,4] B. A. Brown,[2,1] A. A. Chen,[5] K. A. Chipps,[6,7,8] N. Cooper,[9] D. Irvine,[5] E. McNeice,[5] F. Montes,[1,10] F. Naqvi,[9] R. Ortez,[2,1,11] S. D. Pain,[7] J. Pereira,[1,10] C. J. Prokop,[3,1] J. Quaglia,[12,10,1] S. J. Quinn,[2,1,10] J. Sakstrup,[2,1] M. Santia,[2,1] S. B. Schwartz,[2,1,13] S. Shanab,[2,1] A. Simon,[1,14] A. Spyrou,[2,1,10] and E. Thiagalingam[5]

[1]*National Superconducting Cyclotron Laboratory, Michigan State University, East Lansing, Michigan 48824, USA*
[2]*Department of Physics and Astronomy, Michigan State University, East Lansing, Michigan 48824, USA*
[3]*Department of Chemistry, Michigan State University, East Lansing, Michigan 48824, USA*
[4]*Physics Department, Kalamazoo College, Kalamazoo, Michigan 49006, USA*
[5]*Department of Physics and Astronomy, McMaster University, Hamilton, Ontario L8S 4M1, Canada*
[6]*Department of Physics, Colorado School of Mines, Golden, Colorado 08401, USA*
[7]*Physics Division, Oak Ridge National Laboratory, Oak Ridge, Tennessee 37831, USA*
[8]*Department of Physics and Astronomy, University of Tennessee, Knoxville, Tennessee 37996, USA*
[9]*Department of Physics and Wright Nuclear Structure Laboratory, Yale University, New Haven, Connecticut 06520, USA*
[10]*Joint Institute for Nuclear Astrophysics, Michigan State University, East Lansing, Michigan 48824, USA*
[11]*Department of Physics, University of Washington, Seattle, Washington 98195, USA*
[12]*Department of Electrical Engineering, Michigan State University, East Lansing, Michigan 48824, USA*
[13]*Geology and Physics Department, University of Southern Indiana, Evansville, Indiana 47712, USA*
[14]*Department of Physics and Joint Institute for Nuclear Astrophysics, University of Notre Dame, Notre Dame, Indiana 46556, USA*

(Dated: May 30, 2016)

Background: Measurements of β decay provide important nuclear structure information that can be used to probe isospin asymmetries and inform nuclear astrophysics studies.

Purpose: To measure the β–delayed γ decay of ^{26}P and compare the results with previous experimental results and shell model calculations.

Method: A ^{26}P fast beam produced using nuclear fragmentation was implanted into a planar germanium detector. Its β–delayed γ–ray emission was measured with an array of 16 high-purity germanium detectors. Positrons emitted in the decay were detected in coincidence to reduce the background.

Results: The absolute intensities of ^{26}P β-delayed γ-rays were determined. A total of six new β–decay branches and 15 new γ–ray lines have been observed for the first time in ^{26}P β–decay. A complete β–decay scheme was built for the allowed transitions to bound excited states of ^{26}Si. ft values and Gamow-Teller strengths were also determined for these transitions and compared with shell model calculations and the mirror β–decay of ^{26}Na, revealing significant mirror asymmetries.

Conclusions: A very good agreement with theoretical predictions based on the USDB shell model is observed. The significant mirror asymmetry observed for the transition to the first excited state ($\delta = 51(10)\%$) may be evidence for a proton halo in ^{26}P.

PACS numbers: 23.40.-s,23.20.Lv,27.30.+t,26.30-k

I. INTRODUCTION

The detailed study of unstable nuclei has been a major subject in nuclear physics during recent decades. β decay measurements provide not only important information on the structure of the daughter and parent nuclei, but can also be used to inform nuclear astrophysics studies and probe fundamental subatomic symmetries [1]. The link between experimental results and theory is given by the reduced transition probabilities, ft. Experimental ft values involve three measured quantities: the half-life, $t_{1/2}$, the Q value of the transition, which determines the statistical phase space factor f, and the branching ratio associated with that transition, BR.

In the standard $\mathcal{V}$–$\mathcal{A}$ description of β decay, ft values are related to the fundamental constants of the weak interaction and the matrix elements through this equation:

$$ft = \frac{\mathcal{K}}{g_V^2|\langle f|\tau|i\rangle|^2 + g_A^2|\langle f|\sigma\tau|i\rangle|^2}, \quad (1)$$

where $\mathcal{K}$ is a constant and $g_{V(A)}$ are the vector (axial) coupling constants of the weak interaction; σ and τ are the spin and isospin operators, respectively. Thus, a comparison of the experimental ft values with the theoretical ones obtained from the calculated matrix elements is a good test of the nuclear wave functions obtained with model calculations. However, in order to reproduce the ft values measured experimentally, the axial-vector cou-

* perezlou@nscl.msu.edu
† wrede@nscl.msu.edu

pling constant g_A involved in Gamow-Teller transitions has to be renormalized [2, 3]. The effective coupling constant $g'_A = q \times g_A$ is deduced empirically from experimental results and depends on the mass of the nucleus: the quenching factor is $q = 0.820(15)$ in the p shell [4], $q = 0.77(2)$ in the sd shell [5] and $q = 0.744(15)$ in the pf shell [6]. Despite several theoretical approaches attempting to reveal the origin of the quenching factor it is still not fully understood [7].

Another phenomenon which shows the limitations of our theoretical models is the so-called *β–decay mirror asymmetry*. If we assume that the nuclear interaction is independent of isospin, the theoretical description of β decay is identical for the decay of a proton (β^+) or a neutron (β^-) inside a nucleus. Therefore, the ft values corresponding to analog transitions should be identical. Any potential asymmetries are quantified by the asymmetry parameter $\delta = ft^+/ft^- - 1$, where the $ft^\pm$ refers to the $\beta^\pm$ decays in the mirror nuclei. The average value of this parameter is $(4.8 \pm 0.4)\%$ for p and sd shell nuclei [8]. From a theoretical point of view the mirror asymmetry can have two origins: a) the possible existence of exotic *second-class currents* [9–11], which are not allowed within the framework of the standard $\mathcal{V}$–$\mathcal{A}$ model of the weak interaction and b) the breaking of the isospin symmetry between the initial or final nuclear states. Shell-Model calculations were performed to test the isospin non-conserving part of the interaction in β decay [12]. The main contribution to the mirror asymmetry due to nuclear structure was found to be from the difference in the matrix elements of the Gamow-Teller operator ($|\langle f|\sigma\tau|i\rangle|^2$), due to isospin mixing and/or differences in the radial wave functions.

Large mirror asymmetries have been reported for transitions involving halo states [13]. For example, the asymmetry parameter for the $A = 17$ mirror decays ^{17}Ne$\rightarrow^{17}$F and ^{17}N$\rightarrow^{17}$O to the first excited states of the respective daughters has been measured to be $\delta = (-55 \pm 9)\%$ and $\delta = (-60 \pm 1)\%$ in two independent experiments [14, 15]. This result has been interpreted as evidence for a proton halo in the first excited state of ^{17}F assuming that the fraction of $2s_{1/2}$ component of the valence nucleons remains the same in ^{17}Ne and ^{17}N. However, a different interpretation was also given in terms of charge dependent effects which increase the $2s_{1/2}$ fraction in ^{17}Ne by about 50% [16]. The latter result is also consistent with the high cross section obtained in the fragmentation of ^{17}Ne [17, 18], suggesting the existence of a halo in ^{17}Ne. More recently Kanungo *et al.* reported the possiblity of a two-proton halo in ^{17}Ne [19]. An extremely large mirror asymmetry was also observed in the mirror decay of $A = 9$ isobars ^{9}Li$\rightarrow^9$Be and ^{9}C$\rightarrow^9$B. A value of $\delta = (340 \pm 70)\%$ was reported for the ^{9}Li and ^{9}C β–decay transitions to the 11.8 and 12.2 MeV levels of their respective daughters, which is the largest ever measured [20, 21]. Despite the low experimental interaction cross sections measured with various targets in attempts to establish the halo nature of ^{9}C [18, 22], recent results at intermediate energies [23], together with the anomalous magnetic moment [24] and theoretical predictions [25–27], make ^{9}C a proton halo candidate. The potential relationship between large mirror asymmetries and halos is therefore clear. Precision measurements of mirror asymmetries in states involved in strong, isolated, β–decay transitions might provide a technique to probe halo nuclei that is complementary to total interaction cross section and momentum distribution measurements in knockout reactions [13].

Moreover, β decay of proton-rich nuclei can be used for nuclear astrophysics studies. Large Q_β-values of these nuclei not only allow the population of the bound excited states of the daughter, but also open particle emission channels. Some of these levels correspond to astrophysically significant resonances which cannot be measured directly due to limited radioactive beam intensities. For example, the ^{25}Al$(p,\gamma)^{26}$Si reaction [28] plays an important role in the abundance of the cosmic γ-ray emitter ^{26}Al. The effect of this reaction is to reduce the amount of ground state ^{26}Al, which is bypassed by the sequence ^{25}Al$(p,\gamma)^{26}$Si$(\beta\nu)^{26m}$Al, reducing therefore the intensity of the 1809-keV γ–ray line characteristic of the ^{26}Al β decay [29]. Thus it is important to constrain the ^{25}Al$(p,\gamma)^{26}$Si reaction rate.

^{26}P is the most proton-rich bound phosphorus isotope. With a half-life of 43.7(6) ms and a Q_{EC} value of 18258(90) keV [8] the β decay can be studied over a wide energy interval. β-delayed γ–rays and protons from excited levels of ^{26}Si below and above the proton separation energy of 5513.8(5) keV [30] were observed directly in previous experiments [8, 31, 32] and, more recently, indirectly from the Doppler broadening of peaks in the β-delayed proton–γ spectrum [33]. The contribution of novae to the abundance of ^{26}Al in the galaxy has been recently constrained by using experimental data on the β decay of ^{26}P [34].

In addition, ^{26}P is a candidate to have a proton halo [27, 35–37]. Phosphorus isotopes are the lightest nuclei expected to have a ground state with a dominant contribution of a $\pi s_{1/2}$ orbital. Low orbital angular momentum orbitals enhance the halo effect, since higher ℓ-values give rise to a confining centrifugal barrier. The low separation energy of ^{26}P (143(200) keV [30], 0(90) keV[8]), together with the narrow momentum distribution and enhanced cross section observed in proton-knockout reactions [38] give some experimental evidence for the existence of a proton halo in ^{26}P.

In this paper, we present a comprehensive summary of the β-delayed γ decay of ^{26}P measured at the National Superconducting Cyclotron Laboratory (NSCL) at Michigan State University during a fruitful experiment for which selected results have already been reported in two separate shorter papers [33, 34]. In the present work, the Gamow–Teller strength, $B(GT)$, and the experimental ft values are compared to theoretical calculations and to the decay of the mirror nucleus ^{26}Na to investigate the Gamow-Teller strength and mirror asymmetry, re-

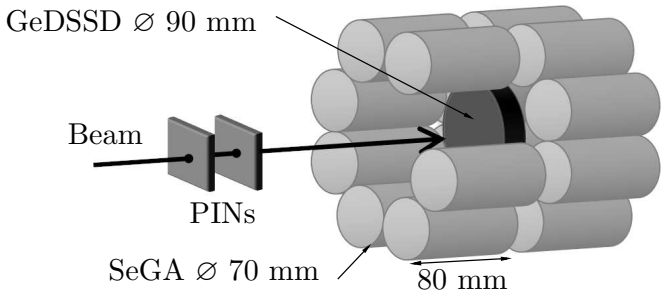

FIG. 1. Schematic view of the experimental setup. The thick arrow indicates the beam direction. One of the 16 SeGA detectors has been removed to show the placement of the GeDSSD.

spectively. A potential relationship between the mirror asymmetry and the existence of a proton halo in ^{26}P is also discussed. Finally, in the last section, the calculated thermonuclear ^{25}Al$(p,\gamma)^{26}$Si reaction rate, which was used in Ref. [34] to estimate the contribution of novae to the abundance of galactic ^{26}Al, is tabulated for completeness.

II. EXPERIMENTAL PROCEDURE

The experiment was carried out at the National Superconducting Cyclotron Laboratory (NSCL). A 150 MeV/u 75 pnA primary beam of ^{36}Ar was delivered from the Coupled Cyclotron Facility and impinged upon a 1.55 g/cm^2 Be target. The ^{26}P ions were in-flight separated from other fragmentation products according to their magnetic rigidity by the A1900 fragment separator [39]. The Radio-Frequency Fragment Separator (RFFS) [40] provided a further increase in beam purity before the beam was implanted into a 9 cm diameter, 1 cm thickness planar germanium double–sided strip detector (GeDSSD) [41]. In order to detect signals produced by both the implanted ions and the β particles emitted during the decay, the GeDSSD was connected to two parallel amplification chains. This allowed the different amounts of energy deposited in implantations (low gain) and decays (high gain) to be detected in the GeDSSD. The GeDSSD was surrounded by the high purity germanium detector array SeGA [42] in its barrel configuration which was used to measure the β-delayed γ rays (see Fig.1).

The identification of the incoming beam ions was accomplished using time-of-flight and energy loss signals. The energy loss signals were provided by a pair of silicon PIN detectors placed slightly upstream of the decay station. The time of flight was measured between one of these PINs and a plastic scintillator placed 25 m upstream, at the A1900 focal plane. Figure 2 shows a two-dimensional cluster plot of the energy loss versus the time of flight for the incoming beam taken prior to a re-tune that improved the beam purity substantially for the majority of the experiment. A coincidence condition requiring a low-gain signal in the GeSSD was applied to ensure the ions were implanted in the detector. It shows that the main contaminant in our beam was the radioactive isotone ^{24}Al (∼13%). During the early portion of the experiment, a small component of ^{25}Si was also present in the beam. We estimated its ratio and it was on average 2.1%, but this value was diluted to 0.5% after incorporating the data acquired after the re-tune. Small traces of lighter isotones like ^{22}Na and ^{20}F were also present (∼2.5%). The total secondary beam rate was on average 80 ions/s and the overall purity of the implanted beam was 84%. This value of the beam purity differs from the previous reported values in Ref. [34], in which the implant condition was not applied The ^{26}P component was composed of the ground state and the known 164.4(1) keV isomeric state [43, 44]. Due to the short half-life of the isomer (120(9) ns) [43] and the fact that it decays completely to the ground state of ^{26}P, our β-decay measurements were not affected by it.

The data were collected event-by-event using the NSCL digital acquisition system [45]. Each channel provided its own timestamp signal, which allowed coincidence gates to be built between the different detectors. In order to select β–γ coincidence events, the high-gain energy signals from the GeDSSD were used to indicate that a β decay occurred. The subsequent γ rays emitted from excited states of the daughter nuclei were selected by setting a 1.5-μs coincidence window. The 16 spectra obtained by each of the elements of SeGA were then added together after they were gain matched run-by-run to account for possible gain drifts during the course of

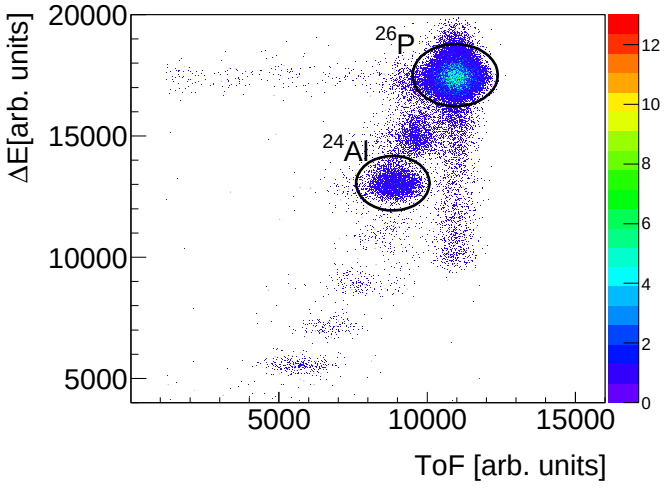

FIG. 2. (Color online) Particle identification plot obtained for a selection of runs during the early portion of the experiment, before the beam tune was fully optimized. The energy loss was obtained from one of the PIN detectors and the time of flight between the same detector and the scintillator placed at the focal plane of the A1900 separator. A low-gain energy signal in the GeDSSD condition was used. The color scale corresponds to the number of ions.

the experiment.

III. DATA ANALYSIS AND EXPERIMENTAL RESULTS

As mentioned in Section I, the data presented in this paper are from the same experiment described in Refs. [33, 34], but independent sorting and analysis routines were developed and employed. The values extracted are therefore slightly different, but consistent within uncertainties. New values derived in the present work are not intended to supersede those from Refs. [33, 34], but rather to complement them. In this section, the analysis procedure is described in detail and the experimental results are presented.

Figure 3 shows the cumulative γ–ray spectrum observed in all the detectors of the SeGA array in coincidence with a β–decay signal in the GeDSSD. We have identified 48 photopeaks, of which 30 are directly related to the decay of ^{26}P. Most of the other peaks were assigned to the β–decay of the main contaminant of the beam, ^{24}Al. Peaks in the spectrum have been labeled by the γ-ray emitting nuclide. 22 of the peaks correspond to ^{26}Si, while 8 of them correspond to β–delayed proton decays to excited states of ^{25}Al followed by γ-ray emission. In this work we will focus on the decay to levels of ^{26}Si as the ^{25}Al levels have already been discussed in Ref. [33].

A. γ-ray Energy Calibration

The energies of the γ–rays emitted during the experiment were determined from a calibration of the SeGA array. As mentioned in Sect. II and in Refs. [33, 34] a gain-matching procedure was performed to align all the signals coming from the 16 detectors comprising the array. This alignment was done with the strongest background peaks, namely the 1460.8 keV line (from the ^{40}K decay) and the 2614.5 keV one (from the ^{208}Tl decay). The gain–matched cumulative spectrum was then absolutely calibrated *in situ* using the well–known energies of the ^{24}Al β–delayed γ–rays emitted by ^{24}Mg, which cover a wide range in energy from 511 keV to almost 10 MeV [46]. In order to account for possible non-linearities in the response of the germanium detectors, a second degree polynomial fit was used as a calibration function. Results of the calibration are shown in Fig. 4. The standard deviation for this fit is 0.3 keV, which includes the literature uncertainties associated with the energies of ^{24}Mg. The systematic uncertainty was estimated from the residuals of room background peaks not included in the fit. The lower panel of Fig. 4 shows that these deviations are below 0.6 keV, with an average of 0.2 keV. Based on this, the systematic uncertainty was estimated to be 0.3 keV.

B. Efficiencies

1. β-particle Efficiency

The β-particle detection efficiency of the GeDSSD can be determined by taking the ratio between the number of counts under a certain photopeak in the β–gated γ–ray singles spectrum and the ungated one. In principle, the β efficiency depends on Q_β. To investigate this effect, we calculated the ratios between the gated and the ungated spectra for all the ^{24}Mg peaks, which have different combinations of Q_β, and found it to be independent of the end-point energy of the β particles, with an average ratio of $\varepsilon_\beta(^{24}\mathrm{Mg}) = (38.6 \pm 0.9)\%$. Because of the different implantation depths for ^{24}Al and ^{26}P (^{24}Al barely penetrates into the GeDSSD), we also calculated the gated/ungated ratios of the strongest peaks of ^{26}Si (1797 keV) and its daughter ^{26}Al (829 keV) obtaining a constant, average, value for the efficiency of $\varepsilon_\beta = (65.2 \pm 0.7)\%$. The singular value for ^{26}Si and ^{26}Al is explained by their common decay point in the GeDSSD.

2. γ-ray Efficiency

In order to obtain precise measurements of the γ–ray intensities, we determined the photopeak efficiency of SeGA. The photopeak efficiency has been studied over a wide energy range between 400 keV and 8 MeV. The results of a GEANT4 [47] Monte-Carlo simulation were compared with the relative intensities of the well-known ^{24}Mg lines used also in the energy calibration. The high energy lines of this beam contaminant made it possible to benchmark the simulation for energies higher than with standard sources. In addition, the comparison of the simulation to data taken offline with absolutely-calibrated ^{154,155}Eu and ^{56}Co sources allowed us to scale the simulation to determine the efficiency at any energy. The scaling factor was 0.91. The statistical uncertainty of this scaling factor was inflated by a scaling factor of $\sqrt{\chi^2/\nu}$ yielding an uncertainty of 1.5%, which was propagated into de the efficiency. The magnitude of this factor is consistent with GEANT4 simulations of the scatter associated with coincidence summing effects [48]. Figure 5 shows the adopted efficiency curve compared to the source data, and the ^{24}Mg peak intensities. The accuracy of this photopeak efficiency was estimated to be $\delta\varepsilon/\varepsilon = 1.5\%$ for energies below 2800 keV and 5% above that energy.

C. γ-ray intensities

The intensities of the γ rays emitted in the β decay of ^{26}P were obtained from the areas of the photopeaks shown in the spectrum of Figure 3. We used an

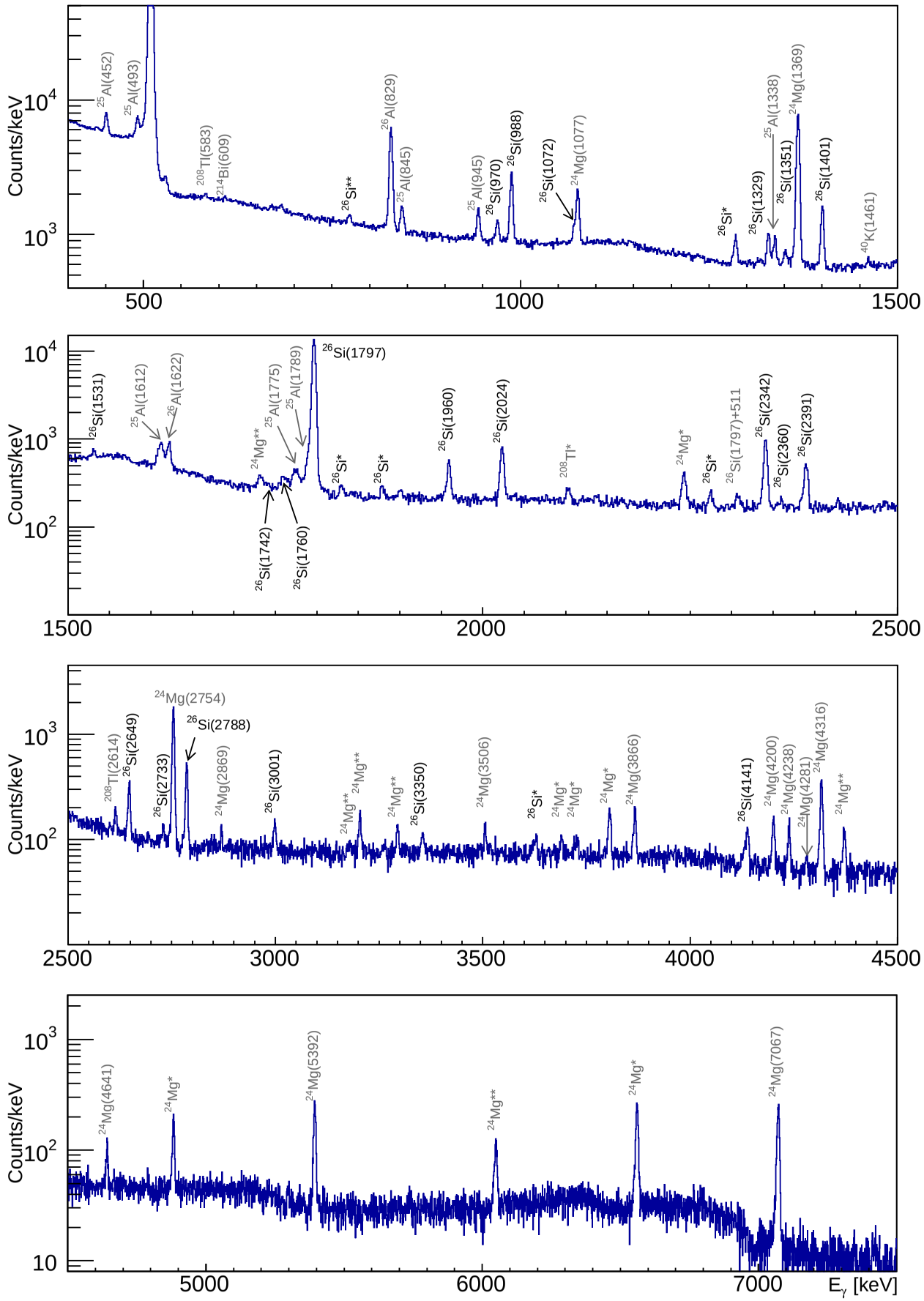

FIG. 3. γ–ray spectrum observed by the SeGA array in coincidence with a β particle in the GeDSSD. Photopeaks have been labeled by the emitting nucleus and its energy rounded to the closest keV integer. Peaks labeled with one (two) asterisks correspond to single (double) escape peaks.

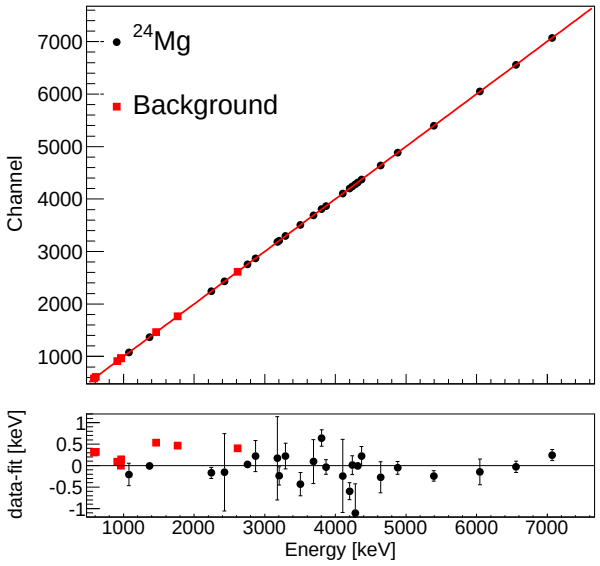

FIG. 4. Upper panel: Energy calibration of SeGA γ–ray spectra using the β–delayed γ rays emitted by ^{24}Al. The solid line is the result of a second degree polynomial fit. Energies and uncertainties are taken from [46]. Lower panel: Residuals of the calibration points with respect to the calibration line.

Exponentially-Modified Gaussian (EMG) function to describe the peak shape together with a linear function to model the local background:

$$F = B + \frac{N}{2\tau} e^{\frac{1}{2\tau}\left(2\mu+\frac{\sigma^2}{\tau}-2x\right)} \mathrm{erfc}\left[\frac{\sigma^2+\tau(\mu-x)}{\sqrt{2}\sigma\tau}\right], \quad (2)$$

where B is a linear background, N is the area below the curve, μ and σ are the centroid and the width of the Gaussian, respectively, and τ is the decay constant of the exponential; erfc is the complementary error function. The parameters describing the width of the Gaussian (σ) and the exponential constant (τ) were determined by fitting narrow isolated peaks at various energies. The centroids and the areas below the peaks were obtained from the fits. When multiple peaks were very close, a multi-peak fitting function was applied using the same values for the τ and σ parameters for all the peaks in the region. In general the fits were very good, with reduced chi-squared (χ^2/ν) close to unity. In those cases where χ^2/ν was bigger than one, the statistical uncertainties were inflated by multiplying them by $\sqrt{\chi^2/\nu}$. Figure 6 shows an example of the fit to the 1960 keV peak.

1. *Absolute normalization*

The total number of ^{26}P ions implanted and subsequently decaying in the GeDSSD is, in principle, needed to obtain an absolute normalization of the γ-ray intensities, and hence the β–branchings of ^{26}Si levels. The number of γ rays observed at energy E is:

$$N_\gamma(E) = N_0 \times \varepsilon_\gamma(E) \times \varepsilon_\beta(E) \times I_\gamma(E) \quad (3)$$

where N_0 is the total number of ions decaying, $\varepsilon_{\gamma(\beta)}$ are the efficiencies to detect γ rays (β particles), and I_γ is the absolute γ–ray intensity. In order to circumvent the uncertainty associated with the total number of ions decaying, we used the ratio of the number of β decays of ^{26}P to its daughter ^{26}Si (61(2)%) [8], and the absolute intensity of the 829-keV γ–rays emitted in the β decay of ^{26}Si, (21.9(5)%) [49], to calculate the intensity of the 1797-keV line, which is the most intense γ ray emitted in the decay of ^{26}P (See Table I). To do so, we applied Eq. (3) to these two γ rays :

$$N_\gamma(829) = N_{^{26}\mathrm{Si}} \varepsilon_\gamma(829)\varepsilon_\beta(829) I_\gamma(829) \quad (4)$$

$$N_\gamma(1797) = N_{^{26}\mathrm{P}} \varepsilon_\gamma(1797)\varepsilon_\beta(1797) I_\gamma(1797) \quad (5)$$

By taking the ratio between Eqs. (4) and (5), the only unknown is the intensity of the 1797-keV γ ray,

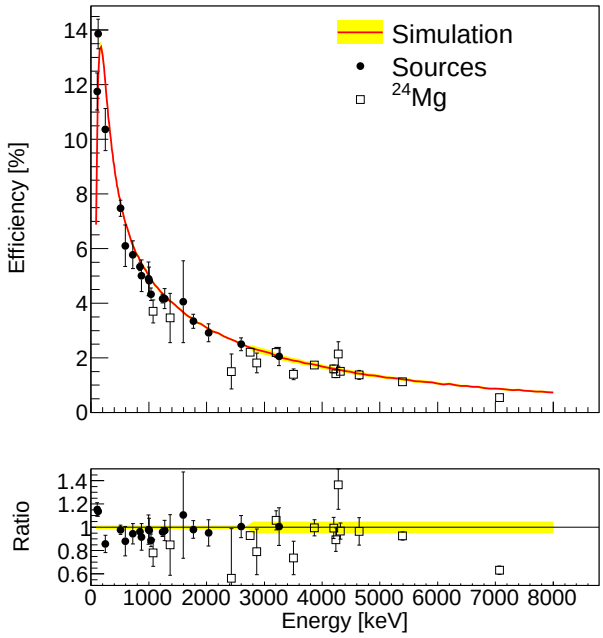

FIG. 5. (Color online) SeGA photopeak efficiency. Top panel: Results of a GEANT4 simulation (solid line, red online) compared to the efficiency measured with absolutely calibrated sources (black circles) and the known ^{24}Mg lines (empty squares). The simulation and the ^{24}Mg data have been scaled to match the source measurements. Bottom panel: Ratio between the simulation and the experimental data. The shaded area (yellow online) shows the adopted uncertainties.

TABLE I. Data on ^{26}Si energy levels and ^{26}P($\beta\gamma$) decay. A total of 12 levels and 22 γ rays have been identified. The first column shows the level energies obtained from the laboratory γ–ray energies shown in the fifth column and include the nuclear recoil correction factor. The second column shows the β–branches. The third and fourth columns show the spin and parity of the initial and final state, respectively. The last column corresponds to the absolute intensities of the γ rays.

E_x (keV)	β–Branch (%)	${}_iJ^\pi_n$	${}_fJ^\pi_n$	E_γ (keV)	I (%)
1797.1(3)	41(3)	2^+_1	0^+_1	1797.1(3)	58(3)
2786.4(3)	<0.39	2^+_2	2^+_1	989.0(3)	5.7(3)
			0^+_1	2786.5(4)[a]	3.4(2)
3756.8(3)	1.9(2)	3^+_1	2^+_2	970.3(3)	1.15(9)
			2^+_1	1959.8(4)	1.7(1)
4138.6(4)	6.2(4)	2^+_3	2^+_2	1352.2(4)[a]	0.48(7)
			2^+_1	2341.2(4)	4.7(3)
			0^+_1	4138.0(5)[a]	1.0(1)
4187.6(4)	4.4(3)	3^+_2	2^+_2	1401.3(3)	3.8(2)
			2^+_1	2390.1(4)[a]	2.2(1)
4445.1(4)	0.8(2)[a]	4^+_1	2^+_2	1660(2)[a]	0.08(6)
			2^+_1	2647.7(5)[a]	1.7(1)
4796.4(5)	0.56(9)[a]	4^+_2	2^+_2	2999.1(5)[a]	0.56(9)
4810.4(4)	3.1(2)[a]	2^+_4	2^+_2	2023.9(3)[a]	3.1(2)
5146.5(6)	0.18(5)[a]	2^+_5	2^+_2	2360.0(6)[a]	0.18(5)
5288.9(4)	0.76(7)[a]	4^+_3	4^+_1	842.9(3)[a]	0.33(7)
			3^+_1	1532.1(5)[a]	0.43(7)
			2^+_1	3491[b]	<0.12[c]
5517.3(3)	2.7(2)[a]	4^+_4	4^+_1	1072.1(5)[a]	0.69(9)
			3^+_2	1329.9(3)[a]	1.4(1)
			3^+_1	1759.7(5)[a]	0.47(6)
			2^+_2	2729.9(5)[a]	0.29(5)
5929.3(6)	0.15(5)[d]	3^+_3	3^+_2	1741.7(9)	0.15(5)

[a] Transition never observed in ^{26}P β decay
[b] Not observed.
[c] 95% confidence level.
[d] Only the γ branch has been measured.

because the β efficiencies can be obtained from the β–gated/ungated ratios discussed in Section II. The value obtained for the intensity of the 1797 keV γ ray is thus 58(3)%, which is in agreement with the value 52(11)% reported in Ref. [8] and more precise. The rest of the γ–ray intensities were determined with respect to this value by employing the efficiency curve and they are presented in Table I. We also report an upper limit on the intensity of one γ ray which was expected to be near the theshold of our sensitivity given the intensity predicted by theory.

D. β–γ–γ coincidences

The 16-fold granularity of SeGA allowed us to obtain β-γ-γ coincidence spectra, which helped to interpret the ^{26}P decay scheme. Figure 7 shows the gamma coincident spectrum gated on the 1797-keV peak, where we can see several peaks corresponding to γ rays detected in coincidence. In order to estimate the background due to random coincidences, we have created another histogram gated on the background close to the peak and normalized to the number of counts within the gated regions. At some energies the background estimate is too high. This is due to a contribution from real γ–γ coincidences involving Compton background, which should not be normalized according to the random assumption.

Figure 8 presents a sample of peaks observed in coincidence when gating on some other intense γ rays observed. From this sample we can see that the coincidence technique helps to cross check the decay scheme. For example Figure 8a shows clearly that the 1401-keV γ ray is emitted in coincidence with the 989-keV γ ray, indicating that the former γ ray comes from a higher-lying level. In the same way, we can see in Fig. 8b that the 1330-keV γ–ray is emitted from a level higher than the 4187 keV level. From the gated spectra, some information can also be extracted from the missing peaks. As Fig. 8c shows, by gating on the 2024-keV γ ray the 970-keV peak disappears, displaying only the 989-keV peak, which means that the 970 keV γ ray comes from a level which is not connected with these two levels by any γ ray cascade. Figure 8d shows clearly the coincidence between the γ ray emitted from the first 2^+ state at 1797 keV to the ground state of ^{26}Si and the 2341-keV γ ray from the third 2^+ state to the first excited state.

These coincidence procedures were systematically analyzed for all possible combinations of γ rays and the

results are summarized in Table II in the form of a 2D matrix, where a checkmark (✓) means the γ rays were detected in coincidence. The condition for a γ ray to be listed in coincidence with another is for it to be at least 3σ above the estimated random-coincidence background. It is worth noting that this background estimate is rather conservative, therefore the significance of some of the peaks is underestimated.

E. Decay scheme of ^{26}P

Figure 9 displays the ^{26}P β-decay scheme deduced from the results obtained in this experiment. Only those levels populated in the β decay are represented. This level scheme was built in a self–consistent way by taking into account the γ–ray energies and intensities observed in the singles spectrum of Fig. 3 and the β–γ–γ coincidence spectra described in Section III D.

The excitation energies of ^{26}Si bound levels, their β–feedings, the energies of the γ rays, and the absolute intensities measured in this work are shown in Table I.

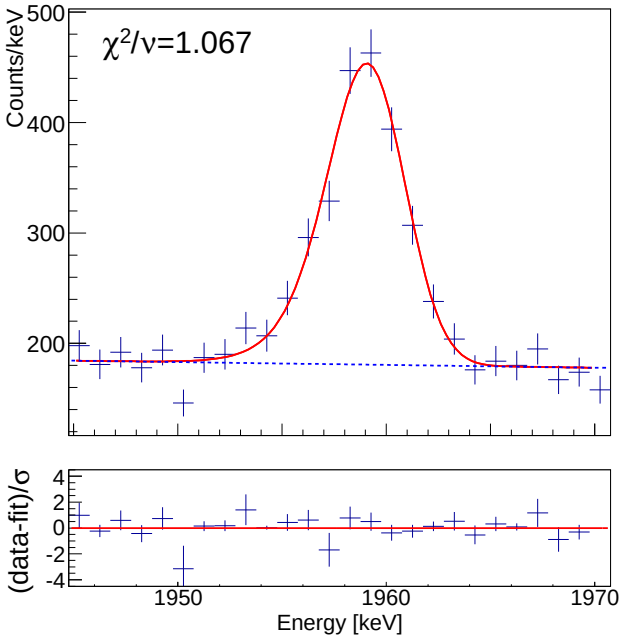

FIG. 6. (Color online)Top panel: Example of a typical fit to the 1960 keV peak, using the function of Eq. 2. The dashed line corresponds to the background component of the fit. Bottom panel: Residuals of the fit in terms of the standard deviation σ.

1. ^{26}Si *level energies, spins and parities*

Level energies of ^{26}Si populated in the β–delayed γ decay of ^{26}P were obtained from the measured γ-ray energies including a correction for the nuclear recoil. The excitation energy values of the levels listed in Table I were obtained from the weighted average of all the possible γ–ray cascades coming from that level. In order to assign spins and parities we compared the deduced level scheme with USDB shell-model calculations and took into account β–decay angular momentum selection rules, showing a 1 to 1 correspondence for all the levels populated by allowed transitions, with a fair agreement in the level energies within theoretical uncertainties of a few hundred keV (see Fig. 9).

2. β–*feedings*

The β branching ratio to the i-th excited energy level can be determined from the γ-ray intensities;

$$BR_i = I_{i,\mathrm{out}} - I_{i,\mathrm{in}}, \tag{6}$$

where $I_{i,\mathrm{out}}(I_{i,\mathrm{in}})$ represents the total γ–ray intensity observed decaying out of (into) the i-th level. The β–decay branches deduced from this experiment are given in Table III, where they are also compared to previous measurements of ^{26}P β decay [8]. In order to investigate the possible missing intensity due to the Pandemonium effect [50], we have used a shell-model calculation to estimate the γ–ray intensities of all possible transitions from bound states feeding each particular level, and found them to be on the order of the uncertainty or (usually) much lower.

IV. DISCUSSION

A. Comparison to previous values of ^{26}Si level energies

We compare in Table IV the energies and the spins and parities deduced in this work with previous values available in the literature [8, 51–53]. The results of Ref. [8] correspond to β decay, thus the same levels are expected to be populated. We observed six levels of ^{26}Si for the first time in the β decay of ^{26}P. These six levels were previously reported using nuclear reactions to populate them [51–53]. The previously reported energies for these levels are in good agreement with the results obtained in this work. However, it is worth mentioning a significant discrepancy (up to 6 keV) with energies obtained in Refs. [51, 53] for the two γ rays emitted from the 4^+_4 state to the 3^+_1 and 2^+_2 states (1759.7 keV and 2729.9 keV, respectively). Despite these discrepancies in the γ–ray energies, the excitation energy of the level reported is in excellent

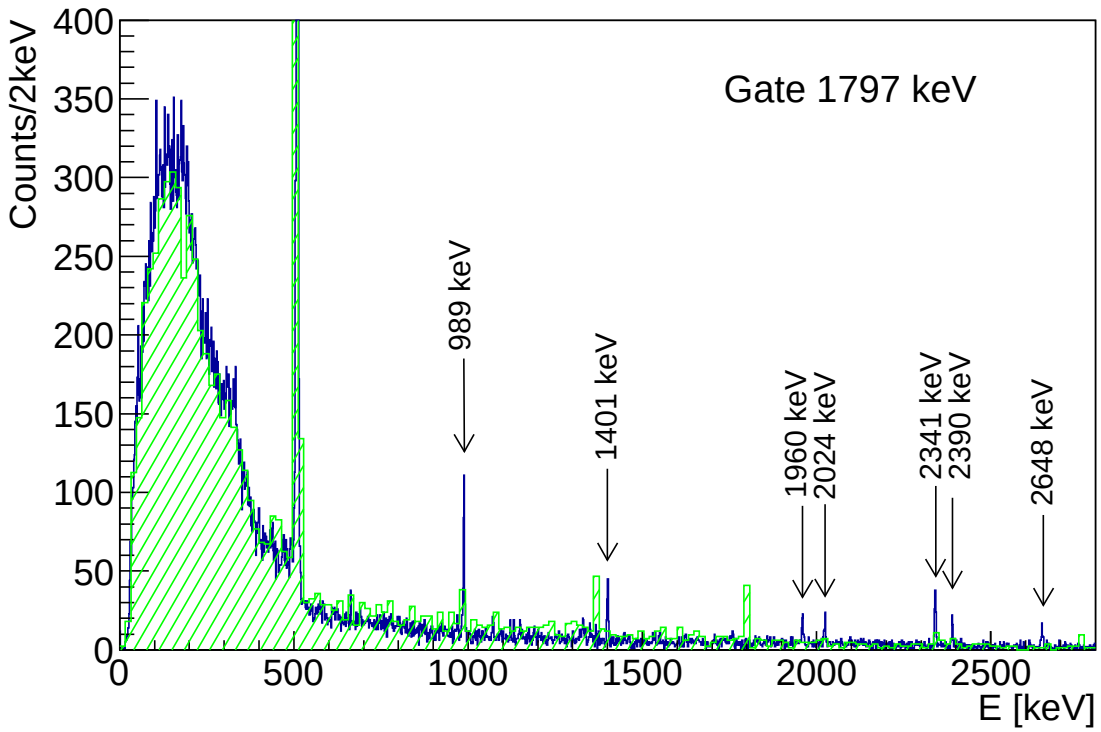

FIG. 7. (Color online) β–γ–γ coincidence spectrum gating on the 1797 keV γ-rays (blue online). The hatched histogram (green online) shows coincidences with continuum background in a relatively broad region above the peak gate. The background bins are 16 keV wide and are normalized to the expected background per 2 keV due to random coincidences. The strongest peaks corresponding to γ rays emitted in coincidence are indicated.

agreement with our results. However, it should be noted that the γ-ray branching ratios are inconsistent for the 1759.7-keV transition.

The 3842-keV level reported in [8] has not been observed in the present work. In agreement with [51–53] we show that this level does not exist, as the 2045-keV γ ray emitted from this level to the first excited state is not seen either in the spectrum of Figure 3 nor the coincidence spectrum with the 1797-keV peak (Fig. 7).

The 4810-keV level was previously tentatively assigned to be a 2^+ state, but this assignment was not clear, because of the proximity to another level at 4830 keV assigned as a 0^+. The fact that the 2024-keV line appears in the spectrum confirms that the spin and parity is $2^+, 3^+$ or 4^+. If this level was 0^+, the β–decay transition which populates this level would be second forbidden ($\Delta J = 3, \Delta\pi = 0$) and highly suppressed.

We observed also the two levels located just above the proton separation energy (S_p = 5513.8 keV). The first one corresponds to a 4^+ state with an energy of 5517 keV. This level was also reported in Refs. [51, 52]. The second level at 5929 keV was previously observed in β–delayed proton emission by Thomas *et al.* [8] and more recently reported in our previous paper describing the present experiment [34]. The results presented here with the same set of data, but with an independent analysis, confirm the evidence for the observation of a γ ray emitted from that level in the present experiment.

B. ft values and Gamow–Teller strength

As mentioned in Section I, the calculation of the experimental ft values requires the measurement of three fundamental quantities: (a) the half-life, (b) the branching-ratio, and (c) the Q value of the decay. The experimental value of the half-life and the semi-empirical Q-value, are $t_{1/2}$ = 43.7(6) ms and Q_{EC} = 18250(90) keV, respectively. Both values were taken from Ref. [8]. The branching ratios from the present work are listed in Table I. The partial half-lives t_i, are thus calculated as:

$$t_i = \frac{t_{1/2}}{BR_i}(1 + P_{EC}), \qquad (7)$$

where BR_i is the β–branching ratio of the i-th level and P_{EC} the fraction of electron capture, which can be neglected for the light nuclide ^{26}P. The statistical phase space factors f were calculated with the parameterization reported in [54] including additional radiative [55] and diffuseness corrections [56]. The uncertainty associated with this calculation is 0.1%, which is added quadrat-

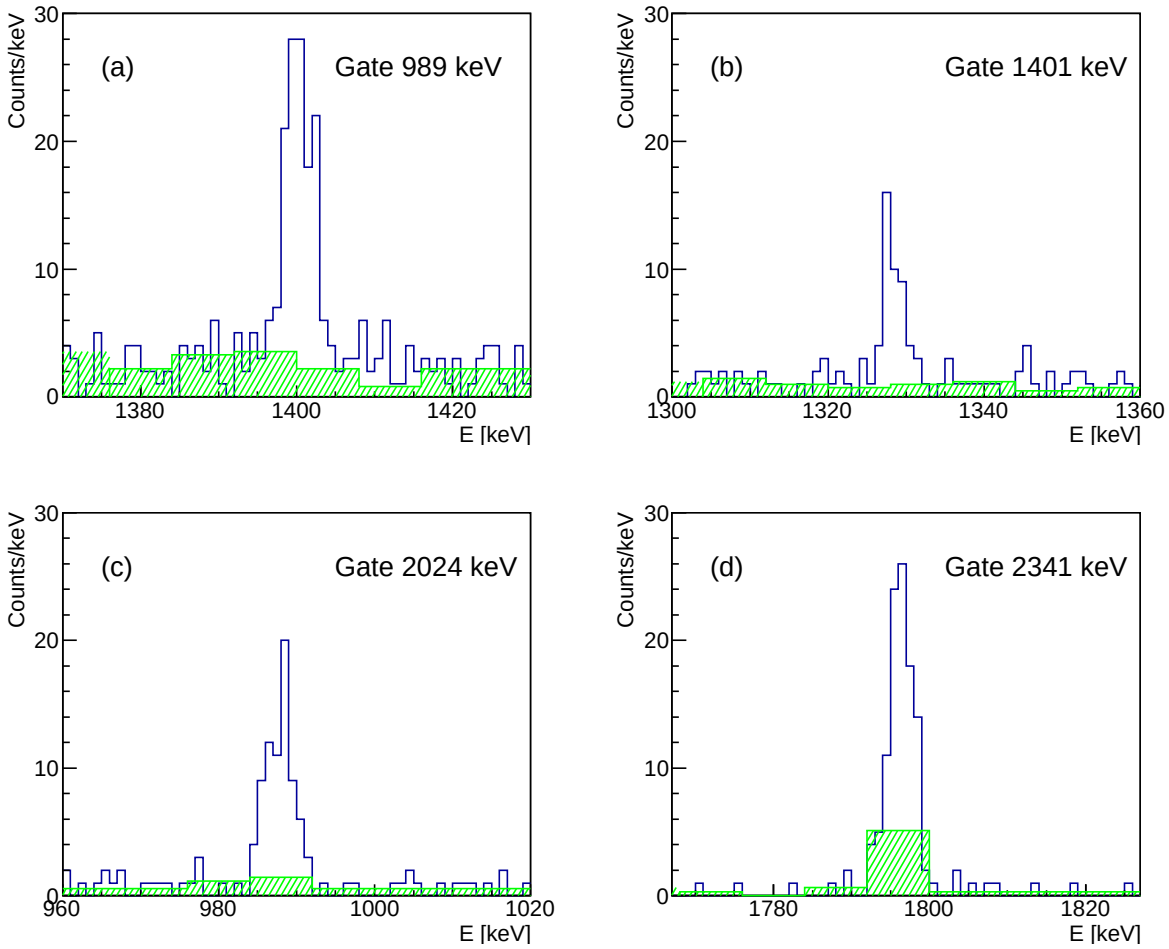

FIG. 8. (Color online) Selected sample of β–γ–γ coincidence peaks gating on different γ-rays: (a)989 keV, (b)1401 keV, (c)2024 keV and (d) 2341 keV. The hatched histogram shows normalized coincidences with continuum background in a relatively broad region above the peak gates. The background bins are 8 keV wide and are normalized to the expected background per keV.

ically to the uncertainty derived from the 0.5% uncertainty of the Q_{EC} value. Table III shows the β-branches and logft values for the transitions to excited levels of ^{26}Si compared to the previous values reported in [8]. For the first excited state, our estimation of the β–feeding is consistent with the previous result. In the case of the second excited state, the previous value is one order of magnitude larger than our upper limit. This is due to the new levels we observed. The large branching ratios observed for the 2_3^+ and the 3_2^+ states compared to previous results, 6.2(4)% and 4.4(3)%, respectively, are noteworthy. The reason for that difference is the observation of new γ–rays emitted by those levels which have now been accounted for. The new levels together with the unobserved state at 3842 keV explain all the discrepancies between the results reported here and literature values [8]. As far as the logft values are concerned the agreement for the first excited state is very good, but when going to higher energies, the discrepancies in the logft values are directly related to those in the branching ratios.

1. *Comparison to theory*

Theoretical calculations were also performed using a shell model code. Wave functions of ^{26}P were deduced using a full *sd*-shell model with the USDB interaction and their corresponding beta decay transitions to ^{26}Si levels.

Figure 9 shows the comparison between the ^{26}Si level energies deduced in this ^{26}P β-decay work to the same levels predicted by the calculation. We observe a fair agreement in the level energies, but the theoretical values are systematically higher. The r.m.s. and maximum deviations between theory and experimental results are 109 keV and 320 keV, respectively. From a direct comparison we also see that in this work we have measured all the states populated in the allowed transitions predicted

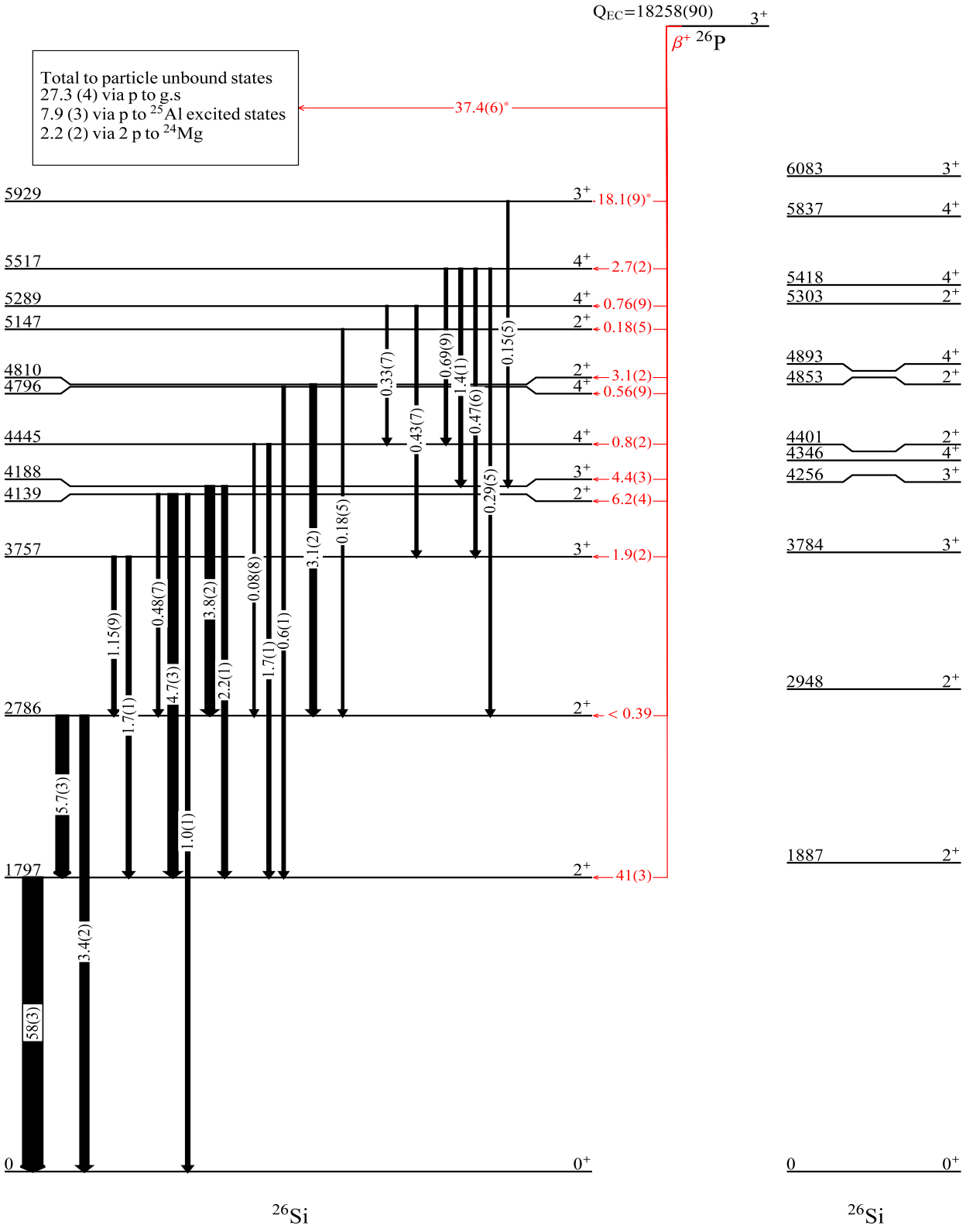

FIG. 9. (Color online) Left: ^{26}P decay scheme as deduced from the experimental data acquired in the present work. γ–ray transition labels correspond to the absolute intensities. β–decay branches corresponding to each populated level are also given (red online). The branches to the unbound 3^+ state and the particle unbound states (asterisks) were taken from literature [8, 33]. Right: ^{26}Si levels populated in ^{26}P β–decay obtained from a USDB shell model calculation. Level energies are given in keV.

TABLE II. Coincidence matrix of all the γ-rays measured in the β–decay of ^{26}P. The first column corresponds to the γ-ray energy on which the gate is set. The following columns indicate the γ rays observed in the gated spectrum. γ–rays observed in coincidence are indicated with a checkmark (✓) if the detection is larger than 3σ above background. γ-ray energies have been rounded to the closest integer and are given in keV.

	843	970	989	1072	1330	1352	1401	1532	1660	1742	1760	1797	1960	2024	2341	2360	2390	2648	2730	2787	2999	4138
843		–	✓	–	–	–	–	–	–	–	–	–	✓	–	–	–	–	✓	–	✓	–	–
970	–		✓	✓	–	–	–	–	–	–	✓	✓	–	–	–	–	–	–	–	–	–	–
989	✓	✓		✓	✓	✓	✓	✓	✓	–	✓	✓	–	✓	–	✓	–	–	✓	✓	–	–
1072	–	–	✓		–	–	✓	–	–	–	–	✓	–	–	–	–	–	✓	–	–	✓	–
1330	–	–	✓	–		–	✓	–	–	–	–	✓	✓	–	–	–	–	–	–	–	–	–
1352	–	–	✓	–	–		–	–	–	–	–	✓	–	–	–	–	–	–	–	✓	–	–
1401	✓	–	✓	✓	✓	–		–	–	✓[a]	–	✓	✓	–	–	–	–	–	–	✓	–	–
1532	✓	✓	✓	—	–	–	–		–	–	–	✓	✓	–	–	–	–	–	–	–	–	–
1660	✓	–	–	✓	–	–	–	–		–	–	✓	–	–	–	–	–	–	–	✓	–	–
1742	–	–	–	–	–	–	✓	–	–		–	–	–	–	–	–	–	–	–	–	–	–
1760	–	✓	✓	–	–	–	–	–	–	–		✓	✓	–	–	–	–	–	–	–	–	–
1797	–	–	✓	–	–	–	✓	–	–	–	–		✓	✓	✓	–	✓	✓	–	–	–	–
1960	✓	–	–	–	✓	–	–	✓	–	–	✓	✓		–	–	–	–	–	–	–	–	–
2024	✓	–	✓	–	–	–	–	–	–	–	–	✓	–		–	–	–	–	–	✓	–	–
2341	–	–	–	–	✓	–	–	–	–	–	–	✓	–	–		–	–	–	–	–	–	–
2360	–	–	–	–	–	–	–	–	–	–	–	✓	–	–	–		–	–	–	✓	–	–
2390	–	–	–	–	✓	–	–	–	–	–	–	✓	–	–	–	–		–	–	–	–	–
2648	✓	–	–	✓	–	–	–	–	–	–	–	✓	–	–	–	–	–		–	–	–	–
2730	–	–	✓	–	–	–	–	–	–	–	–	✓	–	–	–	–	–	–		–	–	–
2787	✓	✓	–	–	✓	✓	✓	–	–	–	✓	–	–	✓	–	–	–	–	–		–	–
2999	–	–	–	–	–	–	–	–	–	–	–	✓	–	–	–	–	–	–	–	–		–
4138	–	–	–	–	–	–	–	–	–	–	–	–	–	–	–	–	–	–	–	–	–	

[a] Not 3σ, but 99.6% C.L.

TABLE III. Comparison of the β–branches and logft values obtained in the present work with previous determinations and shell-model calculations. Values previously unknown are indicated by a dash.

E_x (keV)	β–Branch (%)			logft		
	present Work	Ref. [8]	Theory	present Work	Ref. [8]	Theory
1797	41(3)	44(12)	47.22	4.89(3)	4.89(17)	4.81
2786	<0.39	3.3(20)	0.37	>6.76	5.87(72)	6.77
3757	1.9(2)	2.68(68)	1.17	5.94(4)	5.81(15)	6.135
3842	not obs.	1.68(47)	—	not obs.	6.00(17)	—
4139	6.2(4)	1.78(75)	2.97	5.37(3)	5.93(32)	5.634
4188	4.4(3)	2.91(71)	8.88	5.51(3)	5.71(14)	5.182
4445	0.8(2)	—	1.11	6.23(8)	—	6.071
4796	0.56(9)	—	0.06	6.31(7)	—	7.274
4810	3.1(2)	—	4.45	5.57(3)	—	5.934
5147	0.18(5)	—	0.03	6.7(1)	—	7.474
5289	0.76(7)	—	0.60	6.09(6)	—	6.158
5517	2.7(2)	—	3.96	5.51(4)	—	5.262
5929[a]	0.15(5)[a]	17.96(90)[b]	10.08	6.7(1)[a]	4.60(3)[b]	4.810

[a] Only the γ branch has been measured
[b] Only the proton branch was measured

by the shell-model calculation.

The experimental logft values presented in Table III were determined from the measured branching ratios combined with the known values of Q_{EC} and half-life [8]. Theoretical Gamow-Teller strengths were obtained from the matrix elements of the transitions to states of ^{26}Si populated in the β decay of ^{26}P. In order to compare them to the experimental results, the experimental $B(GT)$ values were calculated from the ft values through the expression

$$B(GT) = \frac{2\mathcal{F}t}{ft}, \tag{8}$$

where $\mathcal{F}t = 3072.27 \pm 0.62$ s [1] is the average corrected ft value from $T = 1\ 0^+ \rightarrow 0^+$ superallowed Fermi

TABLE IV. Excitation energies, spins and parities of ^{26}Si levels from the present work compared to previous γ-ray work and to the allowed ^{26}P($\beta\gamma$) transitions predicted by the shell model. Only the states below 6 MeV are listed. Values not observed are indicated by a dash.

Present work ^{26}P($\beta\gamma$)		Ref. [8] ^{26}P($\beta\gamma$)		Ref. [51] ^{16}O(^{12}C, 2nγ)		Ref. [52] $^{\rm nat}$Mg(^{3}He, nγ)		Ref. [53] ^{24}Mg(^{3}He, nγ)		Theory ^{26}P($\beta\gamma$)	
J^π_n	E_x (keV)	J^π_n	E_x (keV)	J^π_n	E_x (keV)	J^π_n	E_x (keV)	J^π_n	E_x (keV)	J^π_n	E_x (keV)
2^+_1	1797.1(3)	2^+_1	1795.9(2)	2^+_1	1797.3(1)	2^+_1	1797.4(4)	2^+_1	1797.3(1)	2^+_1	1887
2^+_2	2786.4(3)	2^+_2	2783.5(4)	2^+_2	2786.4(2)	2^+_2	2786.8(6)	2^+_2	2786.4(2)	2^+_2	2948
—	—	—	—	0^+_2	3336.4(6)	0^+_2	3335.3(4)	0^+_2	3336.4(2)	—	—
3^+_1	3756.8(3)	(3^+_1)	3756(2)	3^+_1	3756.9(2)	3^+_1	3756.9(4)	3^+_1	3757.1(3)	3^+_1	3784
—	—	(4^+_1)	3842(2)	—	—	—	—	—	—	—	—
2^+_3	4138.6(4)	2^+_3	4138(1)	2^+_3	4139.3(7)	2^+_3	4138.6(4)	2^+_3	4138.8(13)	2^+_3	4401
3^+_2	4187.6(4)	3^+_2	4184(1)	3^+_2	4187.1(3)	3^+_2	4187.4(4)	3^+_2	4187.2(4)	3^+_2	4256
4^+_1	4445.1(4)	—	—	4^+_1	4446.2(4)	4^+_1	4445.2(4)	4^+_1	4445.5(12)	4^+_1	4346
4^+_2	4796.4(5)	—	—	4^+_2	4798.5(5)	4^+_2	4795.6(4)	4^+_2	4796.7(4)	4^+_2	4893
2^+_4	4810.4(4)	—	—	(2^+_4)	4810.7(6)	(2^+_4)	4808.8(4)	2^+_4	4811.9(4)	2^+_4	4853
—	—	—	—	(0^+_3)	4831.4(10)	(0^+_3)	4830.5(7)	0^+_3	4832.1(4)	—	—
2^+_5	5146.5(6)	—	—	2^+_5	5146.7(9)	2^+_5	5144.5(4)	2^+_5	5147.4(8)	2^+_5	5303
4^+_3	5288.9(4)	—	—	4^+_3	5288.2(5)	4^+_3	5285.4(7)	4^+_3	5288.5(7)	4^+_3	5418
4^+_4	5517.3(3)	—	—	4^+_4	5517.2(5)	4^+_4	5517.8(11)	4^+_4	5517.0(5)	4^+_4	5837
—	—	—	—	1^+_1	5677.0(17)	1^+_1	5673.6(10)	1^+_1	5675.9(11)	—	—
—	—	—	—	—	—	0^+_4	5890.0(10)	0^+_4	5890.1(6)	—	—
3^+_3	5929.3(6)	3^+_1	5929(5)[a]	—	—	—	—	—	—	3^+_3	6083

[a] ^{26}P(βp)

β decays. Table V shows the comparison between the experimental and theoretical $B(GT)$ values. A quenching factor $q = 0.77$ ($q^2 = 0.6$) was applied to the shell model calculation [5]. Theoretical predictions overestimate the experimental values for the transitions to the 2^+_1, 3^+_2, 4^+_1, 2^+_4, and 4^+_4 states. Experimental $B(GT)$ values are slightly underestimated for the rest of the states up to 5.9 MeV. The most significant differences are in the 4^+_2 and the 2^+_5 levels for which the predicted $B(GT)$ values differ by almost one order of magnitude with the experimental ones. A possible explanation for this difference is the mixing between different levels.

Figure 10 shows the summed Gamow-Teller strength distribution of the decay of ^{26}P for bound levels up to 5517 keV. In this figure we compare the results obtained in this work with the previous results and the shell-model calculation. We can see that the agreement with the previous experimental results is good for the first excited state, with a small difference that is consistent within uncertainties. As the energy increases the differences become more significant, with our results slightly below the previous ones until the contribution of the new levels is

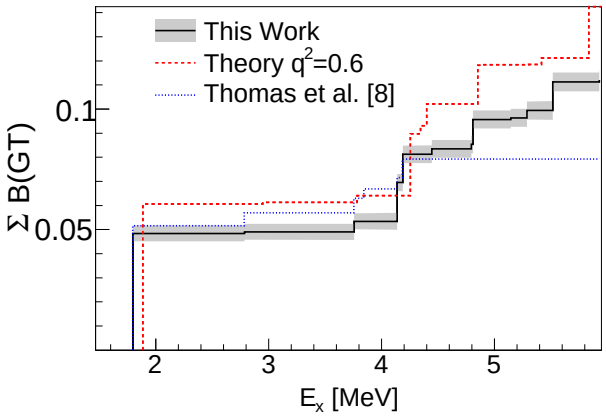

FIG. 10. Summed Gamow-Teller strength distribution of the β decay of ^{26}P up to 5.9 MeV excitation energy. The results of the present experiment are compared to previous results [8] and Shell-Model calculations. A quenching factor $q^2 = 0.6$ was used in the theoretical calculation.

TABLE V. Comparison of the experimental and theoretical $B(GT)$ values obtained in the present work. The quenching factor applied to theory is $q^2 = 0.6$.

Present work			Theory	
E_x (keV)	$B(GT)$	I^π_n	E_x (keV)	$B(GT)$
1797	0.048(3)	2^+_1	1887	0.0606
2786	<0.0007	2^+_2	2948	0.0007
3757	0.0044(4)	3^+_1	3784	0.0029
4139	0.016(1)	2^+_3	4401	0.009
4188	0.0117(1)	3^+_2	4256	0.0256
4445	0.0023(4)	4^+_1	4346	0.0033
4796	0.0018(3)	4^+_2	4893	0.0002
4810	0.0103(7)	2^+_4	4853	0.0161
5147	0.0007(2)	2^+_5	5303	0.0001
5289	0.0031(4)	4^+_3	5418	0.0027
5517	0.012(1)	4^+_4	5837	0.0213

added. For energies above 4.1 MeV, the results from the previous experiment are clearly below our results. If we compare the present data with the theoretical prediction using the typical quenching factor of $q^2 = 0.6$, we see that the theoretical prediction overestimates the summed Gamow-Teller strength in the excitation energy region below 5.9 MeV. If a quenching factor of 0.47 were applied to the shell model calculations instead, the agreement would be almost perfect in this energy region. However, this does not necessarily imply that the value of $q^2 = 0.6$ is inapplicable because only a small energy range has been considered for the normalization. In fact, most of the Gamow-Teller strength is to unbound states which have not been measured in the present work. Furthermore, according to shell model calculations, only ∼21% of the total Gamow-Teller strength is in the Q–value window.

C. Mirror asymmetry and ^{26}P proton halo

The high precision data on the β decay of the mirror-nucleus ^{26}Na from Ref. [57], together with the results obtained in the present work made it possible to calculate finite values of the mirror asymmetry for β-decay transitions from the $A = 26$, $T_z = \pm 2$ mirror nuclei to low lying states of their respective daughters. Table VI shows the results of the ft values obtained for the β decay of ^{26}P and its mirror nucleus, and the corresponding asymmetry parameter, compared to the previous experimental results reported in Ref. [8]. We see that for the low lying states, the agreement between previous data and our results is good, but our results are more precise, yielding the first finite values for this system. For the higher energy states, we report the first values for the mirror asymmetry. We observe large and significant mirror asymmetries with values ranging from −98% up to +100%. As mentioned in Section I, mirror asymmetries can be related to isospin mixing and/or differences in the radial wavefunctions. It was also shown that halo states produce significant mirror asymmetries. The 51(10)% asymmetry observed for the transition to the first excited state could be further evidence for a proton halo in ^{26}P [38]. Higher lying states are not as useful due to possible mixing between nearby states.

In order to investigate this effect more quantitatively, we performed two different shell model calculations with the USDA and USDB interactions. For the transition to the first excited state, these two interactions predict mirror asymmetries of 3% and 2.5%, respectively: far from experimental result. If we lower the energy of the $2s_{1/2}$ proton orbital by 1 MeV in order to account for the low proton separation energy of ^{26}P, the mirror asymmetries we obtain for the first excited state are 60% and 50% for the USDA and USDB interactions, respectively, in agreement with the experimental result and supporting the hypothesis of a halo state [35]. Before firm conclusions can be made, however, more detailed calculations are needed to evaluate the contributions of the other effects that may produce mirror asymmetries.

V. ^{25}Al(p,γ)^{26}Si REACTION RATE CALCULATION

As reported in Ref. [28], the β decay of ^{26}P to ^{26}Si provides a convenient means for determining parameters of the astrophysically relevant reaction ^{25}Al$(p,\gamma)^{26}$Si in novae. In these stellar environments, the nuclei are assumed to have a Maxwell-Boltzmann distribution of energies characterized by the temperature T from which the resonant reaction rate can be described by a sum over the different resonances:

$$\langle \sigma v \rangle = \left(\frac{2\pi}{\mu k T}\right)^{3/2} \hbar^2 \sum_r (\omega\gamma)_r e^{-E_r/kT}, \qquad (9)$$

where $\hbar$ is the reduced Planck constant, k is the Boltzmann constant, μ is the reduced mass and E_r is the energy of the resonance in the center of mass frame. $(\omega\gamma)_r$ is the resonance strength, which is defined as

$$(\omega\gamma)_r = \frac{(2J_r+1)}{(2J_p+1)(2J_{\rm Al}+1)} \left(\frac{\Gamma_p \Gamma_\gamma}{\Gamma}\right)_r . \qquad (10)$$

$J_{r(p,{\rm Al})}$ are the spins of the resonance (reactants), $\Gamma_{p(\gamma)}$ are the proton (γ-ray) partial widths of the resonance and $\Gamma = \Gamma_p + \Gamma_\gamma$ is the total width. It was previously predicted [29] that the levels corresponding to significant resonances at nova temperatures in the ^{25}Al$(p,\gamma)^{26}$Si reaction are the $J^\pi = 1^+_1, 4^+_4, 0^+_4$ and 3^+_3 levels. In our previous work [34] we reported the first evidence for the observation of γ rays emitted from the 3^+_3 level. The determination of the strength of the 3^+_3 resonance in ^{25}Al$(p,\gamma)^{26}$Si based on the experimental measurements of the partial proton width (Γ_p) [58] and the γ–ray branching ratio (Γ_γ/Γ) [34] was also performed and used to determine the amount of ^{26}Al ejected in novae. In this work, we have confirmed the evidence for the 1742-keV γ ray emitted from the 3^+_3 level to the 3^+_2 level in ^{26}Si with an intensity of 0.15(5)%. To some extent, the present paper is a follow-up of our previous work, thus we present here (see Table VII) for completeness the results of the full reaction rate calculation used to obtain the astrophysical results published in [34]. The table shows the total thermonuclear ^{25}Al$(p,\gamma)^{26}$Si reaction rate as a function of temperature including contributions from the relevant resonances, namely $1^+_1, 0^+_4$ and 3^+_3 and the direct capture. For the 1^+ and 0^+ resonances and the direct capture, values are adopted from Ref. [28]. Our table includes the rate limits calculated from a one standard-deviation variation of the parameters.

TABLE VI. Comparison of experimental ft values for the β decay of ^{26}P and its mirror ^{26}Na [57]. The mirror asymmetry δ is also listed and compared to the previous experimental results [8], where applicable.

^{26}P($\beta\gamma$)^{26}Si			^{26}Na($\beta\gamma$)^{26}Mg [57]		δ(%)	
^{26}Si E_x (keV)	ft^+ (s)	I_n^π	^{26}Mg E_x (keV)	ft^- (s)	Present work	Ref.[8]
1797	$7.9(5)\times10^4$	2_1^+	1809	$5.23(2)\times10^4$	51(10)	50(60)
3757	$8.7(8)\times10^5$	3_1^+	3941	$7.5(2)\times10^5$	16(11)	10(40)
4139	$2.4(2)\times10^5$	2_3^+	4332	$4.22(9)\times10^5$	−43(5)	110(160)
4188	$3.2(2)\times10^5$	3_2^+	4350	$2.16(4)\times10^5$	50(10)	110(70)
4445	$1.7(7)\times10^6$	4_1^+	4319	$1.43(3)\times10^6$	20(50)	
4796	$2.1(3)\times10^6$	4_2^+	4901	$1.63(7)\times10^6$	29(18)	
4810	$3.7(3)\times10^5$	2_4^+	4835	$1.85(2)\times10^5$	100(16)	
5147	$5.6(20)\times10^6$	2_5^+	5291	$2.0(3)\times10^7$	−72(11)	
5289	$1.2(2)\times10^6$	4_3^+	5476	$7.9(40)\times10^7$	−98(1)	
5517	$3.2(3)\times10^5$	4_4^+	5716	$1.71(3)\times10^5$	87(18)	

VI. CONCLUSIONS

We have measured the absolute γ-ray intensities and deduced the β–decay branches for the decay of ^{26}P to bound states and low-lying resonances of ^{26}Si. We have observed 6 new β–decay branches and 15 γ–ray lines never observed before in ^{26}P β decay, likely corresponding to most of all the allowed Gamow-Teller transitions between the ground state and 5.9 MeV. The energies measured for the excited states show good agreement with previous results obtained using various nuclear reactions to populate these states. We have calculated the logft values of all these new transitions and compared them to USDB shell model calculations. The reported values show good agreement with the theoretical calculations. In addition, the Gamow-Teller strength function has been calculated and compared to theoretical values, showing that the summed Gamow Teller strength is locally overestimated with the standard *sd* shell quenching of 0.6. The mirror asymmetry was also investigated by calculating the β-decay asymmetry parameter δ for 10 transitions. The significant asymmetries observed, particularly for the transition to the first excited states of ^{26}Si and its mirror ^{26}Mg ($\delta = (51 \pm 10)\%$) might be further evidence for the existence of a proton halo in the ^{26}P. Finally, we have tabulated the total ^{25}Al$(p,\gamma)^{26}$Si reaction rate at nova temperatures used to estimate the galactic production of ^{26}Al in novae in Ref. [34].

ACKNOWLEDGMENTS

The authors gratefully acknowledge the contributions of the NSCL staff. This work is supported by the U.S. National Science Foundation under grants PHY-1102511, PHY-0822648, PHY-1350234, PHY-1404442, the U.S. Department of Energy under contract No. DE-FG02-97ER41020, the U.S. National Nuclear Security Agency under contract No. DE-NA0000979 and the Natural Sciences and Engineering Research Council of Canada.

TABLE VII. Thermonuclear $^{25}\mathrm{Al}(p,\gamma)^{26}\mathrm{Si}$ reaction rate, $N_A\langle\sigma v\rangle$, in units of $\mathrm{cm}^3\mathrm{s}^{-1}\mathrm{mol}^{-1}$ as a function of stellar temperature T, including resonant capture contributions from resonances and direct capture. The first and last columns labeled "Low" and "High", respectively, correspond to the 1 standard deviation uncertainty limits, while the "Central" one corresponds to the recommended rate.

T (GK)	Low	Central	High
0.01	1.10×10^{-37}	1.57×10^{-37}	2.04×10^{-37}
0.015	7.00×10^{-32}	1.00×10^{-31}	1.30×10^{-31}
0.02	3.19×10^{-28}	4.56×10^{-28}	5.93×10^{-28}
0.03	1.23×10^{-23}	1.75×10^{-23}	2.28×10^{-23}
0.04	9.42×10^{-21}	1.34×10^{-20}	1.75×10^{-20}
0.05	1.40×10^{-18}	1.93×10^{-18}	2.88×10^{-18}
0.06	1.16×10^{-16}	2.42×10^{-16}	6.17×10^{-16}
0.07	5.64×10^{-15}	1.50×10^{-14}	4.30×10^{-14}
0.08	1.27×10^{-13}	3.59×10^{-13}	1.06×10^{-12}
0.09	1.46×10^{-12}	4.23×10^{-12}	1.25×10^{-11}
0.1	1.03×10^{-11}	3.01×10^{-11}	8.95×10^{-11}
0.11	5.06×10^{-11}	1.48×10^{-10}	4.40×10^{-10}
0.12	1.99×10^{-10}	5.53×10^{-10}	1.64×10^{-09}
0.13	5.80×10^{-10}	1.68×10^{-09}	4.98×10^{-09}
0.14	1.55×10^{-09}	4.36×10^{-09}	1.28×10^{-08}
0.15	4.04×10^{-09}	1.03×10^{-08}	2.92×10^{-08}
0.16	1.14×10^{-08}	2.43×10^{-08}	6.24×10^{-08}
0.17	3.46×10^{-08}	6.23×10^{-08}	1.34×10^{-07}
0.18	1.02×10^{-07}	1.79×10^{-07}	3.14×10^{-07}
0.19	2.84×10^{-07}	5.41×10^{-07}	8.44×10^{-07}
0.2	7.80×10^{-07}	1.60×10^{-06}	2.42×10^{-06}
0.21	2.07×10^{-06}	4.47×10^{-06}	6.75×10^{-06}
0.22	5.21×10^{-06}	1.15×10^{-05}	1.75×10^{-05}
0.23	1.23×10^{-05}	2.76×10^{-05}	4.21×10^{-05}
0.24	2.72×10^{-05}	6.17×10^{-05}	9.40×10^{-05}
0.25	5.67×10^{-05}	1.29×10^{-04}	1.97×10^{-04}
0.26	1.12×10^{-04}	2.55×10^{-04}	3.89×10^{-04}
0.27	2.09×10^{-04}	4.78×10^{-04}	7.30×10^{-04}
0.28	3.74×10^{-04}	8.55×10^{-04}	1.31×10^{-03}
0.29	6.42×10^{-04}	1.47×10^{-03}	2.24×10^{-03}
0.3	1.06×10^{-03}	2.43×10^{-03}	3.71×10^{-03}
0.31	1.70×10^{-03}	3.88×10^{-03}	5.93×10^{-03}
0.32	2.63×10^{-03}	6.01×10^{-03}	9.19×10^{-03}
0.33	3.96×10^{-03}	9.06×10^{-03}	1.39×10^{-02}
0.34	5.82×10^{-03}	1.33×10^{-02}	2.04×10^{-02}
0.35	8.36×10^{-03}	1.91×10^{-02}	2.92×10^{-02}
0.36	1.18×10^{-02}	2.69×10^{-02}	4.10×10^{-02}
0.37	1.62×10^{-02}	3.70×10^{-02}	5.66×10^{-02}
0.38	2.19×10^{-02}	5.01×10^{-02}	7.66×10^{-02}
0.39	2.92×10^{-02}	6.67×10^{-02}	1.02×10^{-01}
0.4	3.83×10^{-02}	8.75×10^{-02}	1.34×10^{-01}
0.42	6.32×10^{-02}	1.44×10^{-01}	2.21×10^{-01}
0.44	9.94×10^{-02}	2.27×10^{-01}	3.47×10^{-01}
0.46	1.50×10^{-01}	3.42×10^{-01}	5.22×10^{-01}
0.48	2.17×10^{-01}	4.96×10^{-01}	7.58×10^{-01}
0.5	3.06×10^{-01}	6.97×10^{-01}	$1.06 \times 10^{+00}$

[1] J. C. Hardy and I. S. Towner, Phys. Rev. C **91**, 025501 (2015).
[2] D. H. Wilkinson, Phys. Rev. C **7**, 930 (1973).
[3] D. Wilkinson, Nucl. Phys. A **209**, 470 (1973).
[4] W.-T. Chou, E. K. Warburton, and B. A. Brown, Phys. Rev. C **47**, 163 (1993).
[5] B. H. Wildenthal, M. S. Curtin, and B. A. Brown, Phys. Rev. C **28**, 1343 (1983).
[6] G. Martínez-Pinedo, A. Poves, E. Caurier, and A. P. Zuker, Phys. Rev. C **53**, R2602 (1996).
[7] B. A. Brown and W. A. Richter, J. Phys.: Conf. Ser. **20**, 145 (2005).
[8] J.-C. Thomas, L. Achouri, J. Äystö, R. Béraud, B. Blank, G. Canchel, S. Czajkowski, P. Dendooven, A. Ensallem, J. Giovinazzo, N. Guillet, J. Honkanen, A. Jokinen, A. Laird, M. Lewitowicz, C. Longour, F. de Oliveira Santos, K. Peräjärvi, and M. Stanoiu, Eur. Phys. J. A **21**, 419 (2004).
[9] D. Wilkinson, Phys. Lett. B **31**, 447 (1970).
[10] K. Kubodera, J. Delorme, and M. Rho, Phys. Rev. Lett. **38**, 321 (1977).
[11] D. Wilkinson, Eur. Phys. J. A **7**, 307 (2000).
[12] N. Smirnova and C. Volpe, Nucl. Phys. A **714**, 441 (2003).
[13] I. Tanihata, H. Savajols, and R. Kanungo, Prog. Part. Nucl. Phys. **68**, 215 (2013).
[14] M. Borge, J. Deding, P. Hansen, B. Jonson, G. M. Pinedo, P. Møller, G. Nyman, A. Poves, A. Ritcher, K. Riisager, and O. Tengblad, Phys. Lett. B **317**, 25 (1993).
[15] A. Ozawa, M. Fujimaki, S. Fukuda, S. Ito, T. Kobayashi, S. Momota, T. Suzuki, I. Tanihata, K. Yoshida, G. Kraus, and G. Münzenberg, J. Phys. G **24**, 143 (1998).
[16] D. J. Millener, Phys. Rev. C **55**, R1633 (1997).
[17] A. Ozawa, T. Kobayashi, H. Sato, D. Hirata, I. Tanihata, O. Yamakawa, K. Omata, K. Sugimoto, D. Olson, W. Christie, and H. Wieman, Phys. Lett. B **334**, 18 (1994).
[18] A. Ozawa, I. Tanihata, T. Kobayashi, Y. Sugahara, O. Yamakawa, K. Omata, K. Sugimoto, D. Olson, W. Christie, and H. Wieman, Nucl. Phys. A **608**, 63 (1996).
[19] R. Kanungo, M. Chiba, S. Adhikari, D. Fang, N. Iwasa, K. Kimura, K. Maeda, S. Nishimura, Y. Ogawa, T. Ohnishi, A. Ozawa, C. Samanta, T. Suda, T. Suzuki, Q. Wang, C. Wu, Y. Yamaguchi, K. Yamada, A. Yoshida, T. Zheng, and I. Tanihata, Phys. Lett. B **571**, 21 (2003).
[20] U. Bergmann, M. Borge, R. Boutami, L. Fraile, H. Fynbo, P. Hornshøj, B. Jonson, K. Markenroth, I. Martel, I. Mukha, T. Nilsson, G. Nyman, A. Oberstedt, Y. Prezado-Alonso, K. Riisager, H. Simon, O. Tengblad, F. Wenander, and K. W. Rolander, Nucl. Phys. A **692**, 427 (2001).
[21] Y. Prezado, U. Bergmann, M. Borge, J. Cederkll, C. Diget, L. Fraile, H. Fynbo, H. Jeppesen, B. Jonson, M. Meister, T. Nilsson, G. Nyman, K. Riisager, O. Tengblad, L. Weissmann, and K. W. Rolander, Phys. Lett. B **576**, 55 (2003).
[22] B. Blank, C. Marchand, M. Pravikoff, T. Baumann, F. Boué, H. Geissel, M. Hellström, N. Iwasa, W. Schwab, K. Sümmerer, and M. Gai, Nucl. Phys. A **624**, 242 (1997).
[23] D. Nishimura *et al.*, Annual Report, Osaka University (2006).
[24] K. Matsuta, M. Fukuda, M. Tanigaki, T. Minamisono, Y. Nojiri, M. Mihara, T. Onishi, T. Yamaguchi, A. Harada, M. Sasaki, T. Miyake, S. Fukuda, K. Yoshida, A. Ozawa, T. Kobayashi, I. Tanihata, J. Alonso, G. Krebs, and T. Symons, Nucl. Phys. A **588**, c153 (1995).
[25] H. Rui, L. Jia-Xing, Y. Jiang-Ming, J. Juan-Xia, W. Jian-Song, and H. Qiang, Chin. Phys. Lett. **27**, 092101 (2010).
[26] K. Varga, Y. Suzuki, and I. Tanihata, Phys. Rev. C **52**, 3013 (1995).
[27] R. K. Gupta, S. Kumar, M. Balasubramaniam, G. Münzenberg, and W. Scheid, J. Phys. G **28**, 699 (2002).
[28] C. Wrede, Phys. Rev. C **79**, 035803 (2009).
[29] C. Iliadis, L. Buchmann, P. M. Endt, H. Herndl, and M. Wiescher, Phys. Rev. C **53**, 475 (1996).
[30] M. Wang, G. Audi, A. Wapstra, F. Kondev, M. MacCormick, X. Xu, and B. Pfeiffer, Chin. Phys. C **36**, 1603 (2012).
[31] M. Cable, J. Honkanen, R. Parry, S. Zhou, Z. Zhou, and J. Cerny, Phys. Lett. B **123**, 25 (1983).
[32] M. D. Cable, J. Honkanen, E. C. Schloemer, M. Ahmed, J. E. Reiff, Z. Y. Zhou, and J. Cerny, Phys. Rev. C **30**, 1276 (1984).
[33] S. B. Schwartz, C. Wrede, M. B. Bennett, S. N. Liddick, D. Pérez-Loureiro, A. Bowe, A. A. Chen, K. A. Chipps, N. Cooper, D. Irvine, E. McNeice, F. Montes, F. Naqvi, R. Ortez, S. D. Pain, J. Pereira, C. Prokop, J. Quaglia, S. J. Quinn, J. Sakstrup, M. Santia, S. Shanab, A. Simon, A. Spyrou, and E. Thiagalingam, Phys. Rev. C **92**, 031302 (2015).
[34] M. B. Bennett, C. Wrede, K. A. Chipps, J. José, S. N. Liddick, M. Santia, A. Bowe, A. A. Chen, N. Cooper, D. Irvine, E. McNeice, F. Montes, F. Naqvi, R. Ortez, S. D. Pain, J. Pereira, C. Prokop, J. Quaglia, S. J. Quinn, S. B. Schwartz, S. Shanab, A. Simon, A. Spyrou, and E. Thiagalingam, Phys. Rev. Lett. **111**, 232503 (2013).
[35] B. Brown and P. Hansen, Phys. Lett. B **381**, 391 (1996).
[36] Z. Ren, B. Chen, Z. Ma, and G. Xu, Phys. Rev. C **53**, R572 (1996).
[37] Y.-J. Liang, Y.-S. Li, Z.-H. Liu, and H.-Y. Zhou, Chin. Phys. Lett. **26**, 032102 (2009).
[38] A. Navin, D. Bazin, B. A. Brown, B. Davids, G. Gervais, T. Glasmacher, K. Govaert, P. G. Hansen, M. Hellström, R. W. Ibbotson, V. Maddalena, B. Pritychenko, H. Scheit, B. M. Sherrill, M. Steiner, J. A. Tostevin, and J. Yurkon, Phys. Rev. Lett. **81**, 5089 (1998).
[39] D. Morrissey, B. Sherrill, M. Steiner, A. Stolz, and I. Wiedenhoever, Nucl. Instr. and Meth. in Phys. Res. B **204**, 90 (2003).
[40] D. Bazin, V. Andreev, A. Becerril, M. Doléans, P. Mantica, J. Ottarson, H. Schatz, J. Stoker, and J. Vincent, Nucl. Instr. and Meth. in Phys. Res. A **606**, 314 (2009).
[41] N. Larson, S. Liddick, M. Bennett, A. Bowe, A. Chemey, C. Prokop, A. Simon, A. Spyrou, S. Suchyta, S. Quinn, S. Tabor, P. Tai, V. Tripathi, and J. VonMoss, Nucl.

Instr. and Meth. in Phys. Res. A **727**, 59 (2013).
[42] W. Mueller, J. Church, T. Glasmacher, D. Gutknecht, G. Hackman, P. Hansen, Z. Hu, K. Miller, and P. Quirin, Nucl. Instr. and Meth. in Phys. Res. A **466**, 492 (2001).
[43] D. Nishimura, M. Fukuda, T. Sakai, M. Tanaka, K. Abe, J. Chiba, S. Fukuda, H. Furuki, A. Homma, H. Hotaka, N. Ichihashi, N. Inaba, K. Iwamoto, T. Izumikawa, Y. Kamisho, K. Kanbe, N. Kikukawa, A. Kitagawa, J. Kouno, M. Nagashima, Y. Nakamura, I. Nishizuka, K. Matsuta, M. Mihara, S. Miyazawa, Y. Morita, J. Ono, T. Ohtsubo, K. Sato, S. Sato, D. Sera, S. Suzuki, S. Suzuki, T. Suzuki, M. Takechi, K. Tashiro, M. Wakabayashi, D. Watanabe, M. Yaguchi, T. Yamaguchi, S. Yamaki, S. Yasumoto, K. Yoshinaga, and Y. Zhu, EPJ Web of Conferences **66**, 02072 (2014).
[44] D. Pérez-Loureiro *et al.*, In preparation.
[45] C. Prokop, S. Liddick, B. Abromeit, A. Chemey, N. Larson, S. Suchyta, and J. Tompkins, Nucl. Instr. and Meth. in Phys. Res. A **741**, 163 (2014).
[46] R. Firestone, Nucl. Data Sheets **108**, 2319 (2007).
[47] S. Agostinelli *et al.*, Nucl. Instr. and Meth. in Phys. Res. A **506**, 250 (2003).
[48] T. M. Semkow, G. Mehmood, P. P. Parekh, and M. Virgil, Nucl. Instr. and Meth. in Phys. Res. A **290**, 437 (1990).
[49] P. Endt, Nucl. Phys. A **633**, 1 (1998).
[50] J. Hardy, L. Carraz, B. Jonson, and P. Hansen, Phys. Lett. B **71**, 307 (1977).
[51] D. Seweryniak, P. J. Woods, M. P. Carpenter, T. Davinson, R. V. F. Janssens, D. G. Jenkins, T. Lauritsen, C. J. Lister, J. Shergur, S. Sinha, and A. Woehr, Phys. Rev. C **75**, 062801 (2007).
[52] T. Komatsubara, S. Kubono, T. Hayakawa, T. Shizuma, A. Ozawa, Y. Ito, Y. Ishibashi, T. Moriguchi, H. Yamaguchi, D. Kahl, S. Hayakawa, D. Nguyen Binh, A. Chen, J. Chen, K. Setoodehnia, and T. Kajino, Eur. Phys. J. A **50**, 136 (2014).
[53] D. T. Doherty, P. J. Woods, D. Seweryniak, M. Albers, A. D. Ayangeakaa, M. P. Carpenter, C. J. Chiara, H. M. David, J. L. Harker, R. V. F. Janssens, A. Kankainen, C. Lederer, and S. Zhu, Phys. Rev. C **92**, 035808 (2015).
[54] D. Wilkinson and B. Macefield, Nucl. Phys. A **232**, 58 (1974).
[55] D. Wilkinson, Nucl. Phys. A **209**, 470 (1973).
[56] D. H. Wilkinson, A. Gallmann, and D. E. Alburger, Phys. Rev. C **18**, 401 (1978).
[57] G. F. Grinyer, C. E. Svensson, C. Andreoiu, A. N. Andreyev, R. A. E. Austin, G. C. Ball, R. S. Chakrawarthy, P. Finlay, P. E. Garrett, G. Hackman, J. C. Hardy, B. Hyland, V. E. Iacob, K. A. Koopmans, W. D. Kulp, J. R. Leslie, J. A. Macdonald, A. C. Morton, W. E. Ormand, C. J. Osborne, C. J. Pearson, A. A. Phillips, F. Sarazin, M. A. Schumaker, H. C. Scraggs, J. Schwarzenberg, M. B. Smith, J. J. Valiente-Dobón, J. C. Waddington, J. L. Wood, and E. F. Zganjar, Phys. Rev. C **71**, 044309 (2005).
[58] P. N. Peplowski, L. T. Baby, I. Wiedenhöver, S. E. Dekat, E. Diffenderfer, D. L. Gay, O. Grubor-Urosevic, P. Höflich, R. A. Kaye, N. Keeley, A. Rojas, and A. Volya, Phys. Rev. C **79**, 032801 (2009).